

Tillandsia usneoides: a successful alternative for biomonitoring changes in air quality due to a new highway in São Paulo, Brazil

Poliana Cardoso-Gustavson¹ · Francine Faia Fernandes² · Edenise Segala Alves³ · Mariana Pereira Victorio³ · Barbara Baesso Moura² · Marisa Domingos³ · Caroline Albuquerque Rodrigues⁴ · Andreza Portella Ribeiro⁵ · Catarina Carvalho Nievola³ · Ana Maria G Figueiredo⁴

Received: 30 July 2015 / Accepted: 16 September 2015 / Published online: 23 September 2015
© Springer-Verlag Berlin Heidelberg 2015

Abstract *Tillandsia usneoides* is an aerial epiphytic bromeliad that absorbs water and nutrients directly from the atmosphere by scales covering its surface. We expanded the use of this species as a broader biomonitor based on chemical and structural markers to detect changes in air quality. The usefulness of such comprehensive approach was tested during the construction and opening of a highway (SP-21) in São Paulo State, Brazil. The biomonitoring study was performed from 2009 to 2012, thus comprising the period during construction and after the highway inauguration. Metal accumulation and

structural alterations were assessed, in addition to microscopy analyses to understand the metal chelation in plant tissues and to assess the causes of alterations in the number and shape of scale cells. Altogether, our analyses support the use of this species as a wide biomonitor of air quality in urbanized areas.

Keywords Atmospheric pollution · Bromeliaceae · Instrumental neutron activation analysis · Metal atmospheric pollution · Mutagenesis · Scale cells

Responsible editor: Constantini Samara

✉ Ana Maria G Figueiredo
anamaria@ipen.br

Poliana Cardoso-Gustavson
cardoso.poliana@ufabc.edu.br

Francine Faia Fernandes
fernandes.francinef@gmail.com

Edenise Segala Alves
ealves@ibot.sp.gov.br

Mariana Pereira Victorio
marip.victorio@gmail.com

Barbara Baesso Moura
bmourabio@gmail.com

Marisa Domingos
momingos@superig.com.br

Caroline Albuquerque Rodrigues
calbuquerque@gmail.com

Andreza Portella Ribeiro
aportellar@yahoo.com.br

Catarina Carvalho Nievola
ccnievola@uol.com.br

- ¹ Centro de Ciências Naturais e Humanas, Universidade Federal do ABC, Rua Arcturus 03, Jardim Antares, São Bernardo do Campo 09606-070, SP, Brazil
- ² Programa de Pós-Graduação em Biodiversidade Vegetal e Meio Ambiente, Instituto de Botânica, Av. Miguel Stefano 3687, Água Funda 04301-902, SP, Brazil
- ³ Núcleo de Pesquisa em Anatomia, Instituto de Botânica, Av. Miguel Stefano 3687, Água Funda 04301-902, SP, Brazil
- ⁴ Laboratório de Análise por Ativação com Nêutrons, Instituto de Pesquisas Energéticas e Nucleares, Av. Prof. Lineu Prestes, 2242, 05508-000 São Paulo, SP, Brazil
- ⁵ Mestrado em Cidades Inteligentes e Sustentáveis, Universidade Nove de Julho, Av. Francisco Matarazzo, 612, prédio C, Água Branca 05001 100, SP, Brazil

Introduction

One of the major sources of heavy metal contamination in urban environments usually comes from particulate matter (PM) emitted by vehicles, including exhaust fumes, oil leaks, wear of tire and breaking discs, and corrosion (Cadle et al. 1997; Janssen et al. 1997; Duong and Lee 2011; Ribeiro et al. 2012; Modrzewska and Wyszowski 2014). However, non-exhausted emissions are presently more important sources of metal pollution than exhaust fumes due to the use of unleaded gasoline and implementation of efficient control measures that have significantly reduced metal emissions. Non-exhausted emissions may contribute to the enrichment of Ba, Cr, Cu, Fe, Ni, Pb, and Zn in road dusts (Duong and Lee 2011; Gunawardana et al. 2012; Thorpe and Harrison 2008; Liu et al. 2014).

Metal emissions can contaminate water, air, and soil, causing adverse effects on both human health and the environment. Saiki et al. (2014), for instance, performed a correlation study between atmospheric heavy metal pollution and cardio-respiratory diseases in São Paulo city, applying a lichenized fungi species (*Canoparmelia texana*) in a passive biomonitoring. These authors found a positive correlation between adult mortality rates and concentrations of Co, Mn, and Zn in the lichen, indicating the usefulness of this biomonitor species for risk prognosis to human populations in such megacity.

Biomonitor plants of metal atmospheric pollution have also been highlighted as a reliable, versatile, and alternative method to extend the routine air quality monitoring programs in metropolitan areas and to improve the air pollution control by governmental agencies (Loppi and Bonini 2000; Monaci et al. 2000; Conti and Cecchetti 2001; Zechmeister et al. 2005). The use of the aerial epiphyte *Tillandsia usneoides* as a biomonitor of metal pollution has been successfully applied in several studies (Vianna et al. 2011; Isaac-Olivé et al. 2012; also, see the revision of the use of *T. usneoides* as biomonitor in several urban cities in Techato et al. (2014), including the metropolitan region of São Paulo (Figueiredo et al. 2007). Mineral concentrations in *T. usneoides* have been usually positively correlated to the aerosol sources in several environmental conditions (Vianna et al. 2011). Some authors have also described in which tissues of this species the metal accumulation occurs. They proved that the adsorption predominates in the scales (a type of non-secretory trichomes usually described in Bromeliaceae species) and is not detected in inner tissues (mesophyll or vascular cells) (Amado Filho et al. 2002; Vianna et al. 2011). The wide area of the scales' surface apparently confers the great capability of *T. usneoides* in holding metals that constitute the particulate matter (Vianna et al. 2011). However, this absence of metals inside leaf tissues suggests the

occurrence of structural components that may retain these metals outside the plant body, thus reducing their harmful effects. In addition, Alves et al. (2008) described and evaluated alterations in the morphology and number of cells that constitute the scales of *T. usneoides* exposed in polluted sites in São Paulo, noticing that the number of anomalous scales correlated positively with ozone concentrations, thus expanding the use of this species to monitoring other atmospheric pollutants. The possible causes of these alterations in both number and shape of epidermal cells, however, is still unknown. Taking into consideration the previous knowledge described, we assumed that a broader biomonitoring method would be based on both metal accumulation and structural alterations in scales. The applicability of such comprehensive and new approach was tested around a peripheral highway recently built in the metropolitan region of São Paulo, in southeast Brazil, the seventh largest urbanized area of the world. This region is characterized by a vehicular fleet of about 8.5 million (DERSA 2015), which is the major source of air pollution. The peripheral highway, regionally known as Rodoanel Mario Covas (SP-21), was built to improve the regional road system linking São Paulo city to several localities in the state and also in the country, with the expectative of reducing the vehicular traffic (DERSA 2015) and consequently the serious environmental and health problems that have been observed in that metropolitan region, due to the particulate matter and other air pollutants, as highlighted by Molina and Molina (2004). The southern part of the peripheral highway, associated to the western one, was particularly built to redirect car and truck traffic coming from São Paulo State and central Brazilian cities to the most important Brazilian port in Santos, therefore avoiding the urban road system of São Paulo city. In contrast, this highway was built and is currently open for routine vehicular traffic in peripheral and less urbanized areas of São Paulo city, which still contains portions of the Atlantic Forest and were less affected by air pollutant impacts before its construction. This new scenario motivated us to verify if the use of *T. usneoides*, applying the mentioned broader approach, would be a convenient alternative (considering both large areas and low cost) for monitoring changes in air quality due to a new source of air pollution. *T. usneoides* was applied as biomonitor of atmospheric pollution during different phases of the construction until the inauguration of the southern part of the peripheral highway. Metal accumulation (Ba, Cr, Cu, Fe, Mo, Ni, Pb, Sb, and Zn) and structural alterations were assessed. In addition, we also developed microscopy analyses to understand (1) the reasons why metals are not absorbed/adsorbed by the

inner tissues of this species, and (2) if the alterations in the number of scale cells result from alterations in cell cycle, an indicative of exposure to mutagenic agents.

Material and methods

Study site and monitoring strategy

The biomonitoring study was performed in the following sites located close to both western and southern portions of the peripheral highway SP-21 (Fig. 1a):

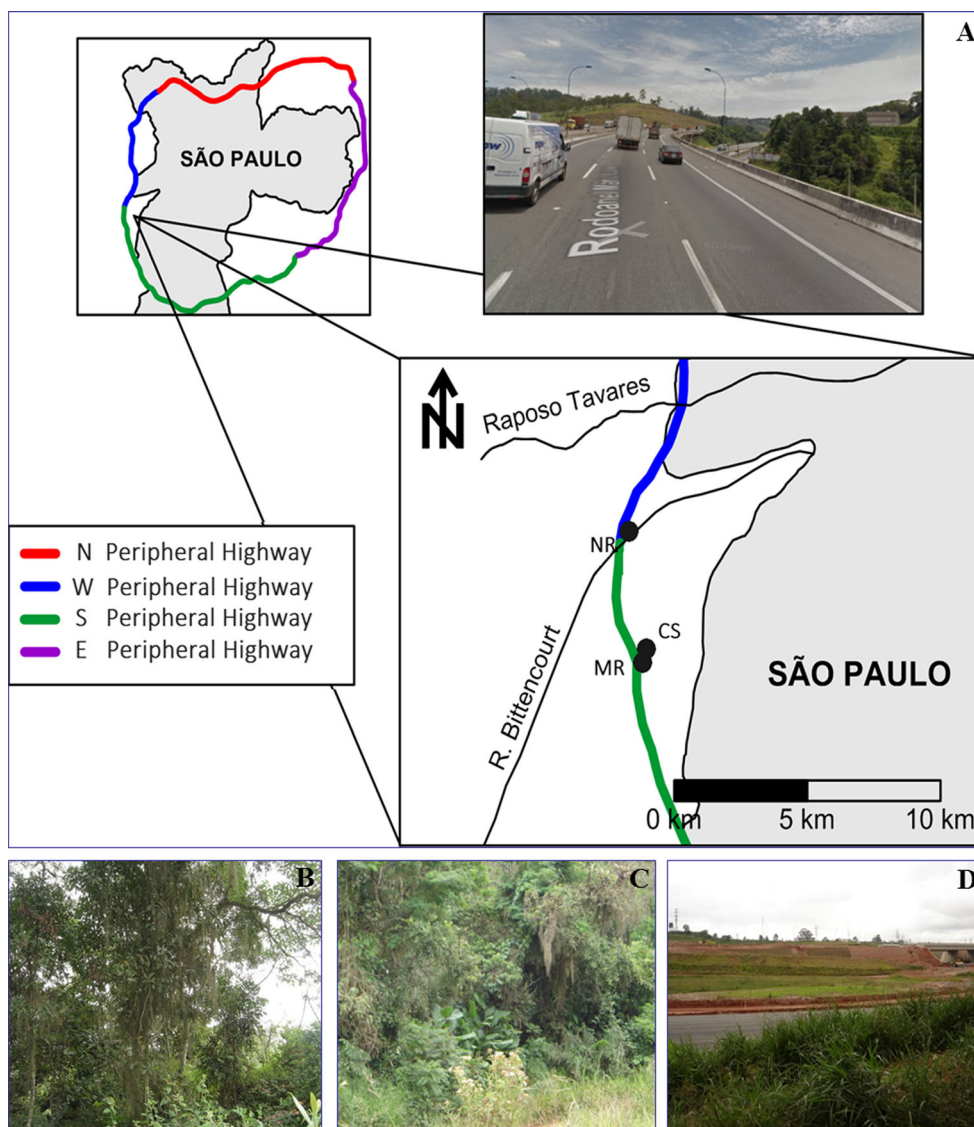
Control site (CS; 23° 40' 05.5" S and 46° 49' 28.1" W; Fig. 1b)—non-urbanized area close to the southern part of SP-21 highway and to a remnant of Atlantic forest. *T. usneoides* was abundant over trees inside and at the border of the forest. Samples collected at this site were used in the

exposure experiments performed at the other sites and also as reference concentration values in analyses metal quantification.

Maintenance road (MR; 23° 40' 21" S and 46° 49' 33" W; Fig. 1c)—it is next to a vicinal road restricted to vehicle traffic during the construction of the southern part of SP-21 highway. Plants were abundant over some trees. *T. usneoides* was abundant in some trees found in this site. This road was deactivated when the highway was opened for routine traffic (April/2010).

New road (NR; 23° 37' 55.1" S and 46° 49' 48.9" W; Fig. 1d)—located about 5 m away from the intersection between the new southern and previously existing western portions of the highway. This portion of the road was opened to vehicular traffic in April/2010 and was increasingly used from that time on. *T. usneoides* plants were not present at this site, thus an active biomonitoring was performed by transplanting samples from the control site to tree branches (1.50 m high),

Fig. 1 The peripheral highway SP-21 (a) and exposure sites: control site (b), maintenance road (c), and new road (d)



maintaining the same isolated conditions of the control site. Part of the transplanted samples was collected for further comparisons, thus representing the time zero (T0). The biomonitoring study was performed from 2009 to 2012, comprising the period during the construction and after the highway inauguration. Table 1 shows the sampling schedule.

Instrumental neutron activation analysis

Samples were dried at 40 °C and then ground using an agate mill to obtain a fine and homogeneous powder. This material was applied in both techniques (INAA and ICP-OES) to metal identification.

Instrumental neutron activation analysis (INAA) technique was applied in the determination the elements Ba, Cr, Mo, Sb, and Zn. Then, 200 mg of *T. usneoides* samples from each collection and biological reference materials, peach leaves (SRM-1547) and mixed polished herbs (MPH-2), were accurately weighed within polyethylene envelopes previously cleaned with diluted nitric acid solution. Samples and standards were irradiated for 16 h at a thermal neutron flux of about 10^{13} n cm⁻²s⁻¹ at the IEA-R1 nuclear reactor of Instituto de Pesquisas Energeticas e Nucleares (IPEN). The measurements of the induced gamma-ray activity were carried out using a GX 20190 hyperpure Ge detector. The multichannel analyzer was an 8192 channel Canberra S-100 plug-in-card in a PC computer. The resolution (FWHM) of the system was 1.90 keV for the 1332 keV gamma-ray of ⁶⁰Co. Two series of measurements were performed after the 16-h irradiation; the first was done from 5–7 days after irradiation and the second one after 15–20 days of decay. Counting times ranged from 3 to 10 h. The gamma-ray spectra were processed by using the in-house gamma-ray software VISPECT. To evaluate the accuracy of data, the biological reference material orchard leaves (SRM 1571) was also analyzed. The coefficient of variation presented a deviation between replicates below 18 % and bias lower than 17 %. The E_n number assures all values in the 95 % confidence interval.

Table 1 Sampling schedule, comprising the period during the construction and after the highway inauguration. April 2010 (T4–T5): opening of the linking of the southern part and western part of the SP-21 highway

Sample collection	Period
T0	Jan/2009
T1 (1st sampling)	Apr/2009
T2 (2nd sampling)	Jun/2009
T3 (3rd sampling)	Nov/2009
T4 (4th sampling)	Mar/2010
T5 (5th sampling)	Aug/2010
T6 (6th sampling)	Nov/2010
T7 (7th sampling)	Feb/2011
T8 (8th sampling)	Apr/2011
T9 (9th sampling)	Feb/2012

Inductively coupled plasma-atomic emission spectrometry

The elements Cu, Ni, and Pb were determined by this technique. Then, 0.6 g of each *T. usneoides* sample was accurately weighed and dissolved in 2 mL HF, 10 mL HNO₃, and 2 mL de H₂O₂ in a closed vessel microwave system (four stages, T_{\max} = 120 °C), as described in Bettinelli et al. (2002). Samples were evaporated to dryness and diluted in HNO₃ 5 % up to 12 mL, and analyzed by inductively coupled plasma-atomic emission spectrometry (ICP-OES) (VARIAN 710 ES). The reference material peach leaves (SRM 1547) was also analyzed to guarantee the accuracy of the data. Results showed bias lower than 10 % and coefficient of variation lower than 12 %. The E_n number obtained exhibited values lower than 1, considered adequate according to the ISO 13258 recommendations (ISO 2005).

Identification and quantification of anomalous scales

Three samples from each exposition site were fixed in FAA₇₀ (Johansen 1940). For tissue dissociation, fragments of the upper region of the leaf were longitudinally sectioned with a razor blade, immersed in a solution of 30 % hydrogen peroxide: glacial acetic acid (1:1 v/v) for 24 h at 60 °C, and washed with distilled water. Fragments were colored with toluidine blue 0.05 % and semi-permanent slides mounted with glycerin: water 1:1. Scales were observed and imaged in a Zeiss Primo Star microscope equipped with a Canon PowerShot A650 IS camera. Quantitative analysis as scale density and index was performed in 30 different fields from each slide (total area of 280 μm²). The scale index was calculated over the stomatal density formula (Salisbury 1927 *apud* Metcalfe and Chalk 1979): number of scales / number of epidermal cells + number of scales × 100. To calculate the percentage of anomalous scales, it was applied the ratio: density of anomalous scales/ (scales density × 100 total).

Fluorescence microscopy of nucleus

Scale cells differentiate rapidly and become lignified and dead when mature, thus being impossible to visualize the nucleus. On the other hand, we had to visualize nucleus of mature cells before cell death process but indeed after finished their divisions, thus with anomaly already established. Thus, we firstly selected anomalous scales from slides used for quantification purposes and then looked for still living cells in which the nucleus were still available to analyze. Slides were dismantled and, after that, samples were rinsed in distilled water, before immersing in a fluorescent nuclear stain, 4',6-diamidino-2-phenylindole (DAPI; 2 mg per mL of distilled water) for 2–3 h at room temperature. Samples were rinsed three times with distilled water to remove excess stain before mounting the leaf apex in distilled water for viewing. Since

scale cells were not in process of divisions, no mitotic figure was visualized, then being possible to compare nucleus size of scale cells with the ones from ordinary epidermis. Samples were observed with a Nikon Eclipse Ti-E epifluorescence microscope with a Hg lamp and a DAPI filter set; images were captured with Nikon NIS Elements software.

Autofluorescence of phenolic compounds

Transversal sections (20 μm thickness) of leaves were cut using a cryomicrotome Leica LM CM1100. Autofluorescence of phenolic compounds was assessed by exciting samples at 364 and 488 nm laser lines and acquiring lambda-stack images (a series of images of the same microscopic region each taken with different wavelengths in 10- to 11-nm increments) from 400 to 600 nm and 490 to 600 nm emissions, respectively. An inverted Zeiss LSM 510-Meta confocal laser scanning microscope was applied to image both glutathione and autofluorescence of phenolic compounds samples using a Zeiss oil immersion objective (×60).

Statistical analyses

The percentage of anomalous scales during the experimental period (T1 to T9) in each site was compared by ANOVA on ranks followed by Dunn’s test. The hierarchical dendrogram obtained by cluster analysis was built from the element concentrations of the control site and new road. Pearson correlation analyses were applied between the average percentage of anomalous scales and heavy metal concentrations in *T. usneoides* exposed in control and polluted sites (maintenance and new roads) during the experimental period.

Results and discussion

Impacts of the SP-21 highway construction

The available data from ARTESP (Press consultancy of the highway consortium) refers to tolled cars that passed through the western part of the highway. The toll began to be collected in August 2011, so these data was available from September 2011. Data from the six first months after the opening of the highway (so starting from zero cars) indicated the passage of 115,767 cars in September 2011, 118,322 in October 2011, 119,409 in November 2011, 124,370 in December 2011, 120,366 in January 2012, and 118,597 in February 2012.

Metal accumulation

Variations of the concentrations of Ba, Cr, Cu, Fe, Mo, Ni, Pb, Sb, and Zn according to the studied sites and exposure time are presented in Fig. 2. The metal concentrations at the control

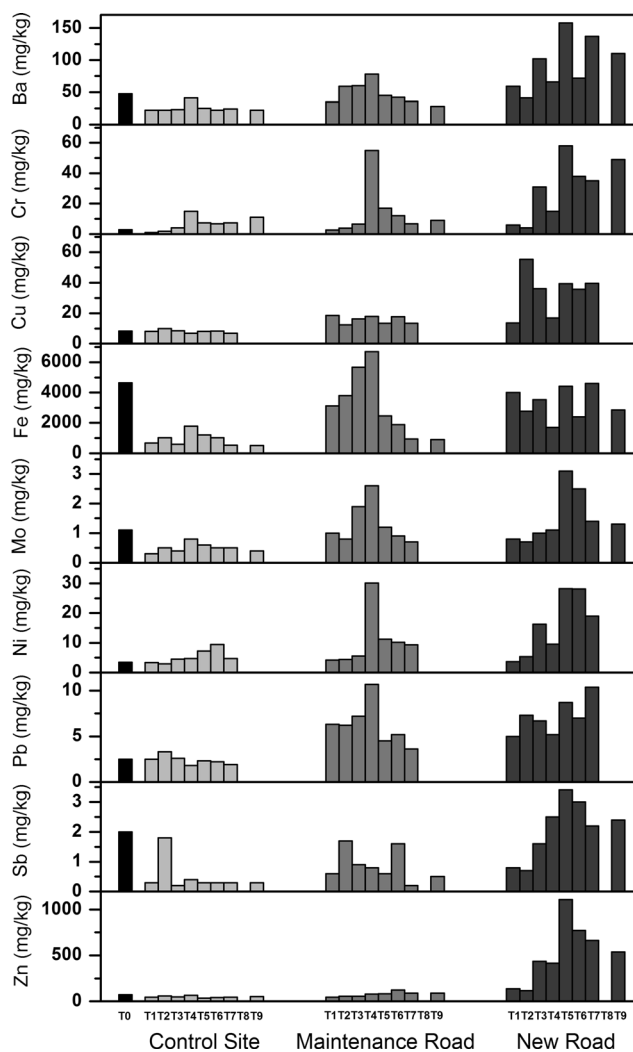


Fig. 2 Element concentrations from *Tillandsia usneoides* plants in relation to the studied sites (*Control Site*, *Maintenance Road*, and *New Road*) and exposure periods (T0–T9)

site were generally lower than those from maintenance and new roads, although some level variations were observed during the exposure time. This fact confirms the potential of *T. usneoides* as bioaccumulator of these metals. Most elements presented a similar tendency of showing higher concentrations at the new road site from the third sampling period and reaching maximum values after the fifth period performed in August 2010. This pattern coincided with the period when the intersection between southern and western portions of the SP-21 highway was opened to routine traffic (April 2010). This site presented a higher vehicle circulation in relation to the other ones. According to DERSA (2015) (traffic department of São Paulo), 1,356,423 vehicles circulated at this road during the first 30 days after the inauguration, in which 70 % of those were cars and 30 % trucks. The *t* test showed a statistical difference ($p < 0.05$) in the concentration values of Cr, Mo, Ni, Pb, Sb, and Zn in plant samples from the new road site before and after the inauguration of the highway. A concentration

enrichment of about ten times was estimated for Cr and Zn in *T. usneoides* from the new road site after the opening of the highway (T5). Ni, Mo, and Sb also showed a significant enrichment after the opening of the highway.

A non-significant variation in the concentrations of Ba, Cu, Fe, and Pb before and after the inauguration of the road indicated that the atmospheric concentration levels of these elements were not influenced by the inauguration of the road. This fact can be visualized in the hierarchical dendrogram obtained by cluster analysis, in which two main groups can be identified (Fig. 3). The first group was divided in two sub-clusters: Sb and Mo constituted the first, while the second one included Ni, Cr, and Zn. The second group was defined by Cu, Fe, Pb, and Ba. These results indicated that Cr and Zn can be applied as metal tracers of traffic-related atmospheric pollution in urban contamination studies. Cr concentrations in the range of 135–1320 mg/kg were reported in car brake dust, while Zn is the most abundant metal in tires (Thorpe and Harrison 2008; Apeagyei et al. 2011). Zinc, in the form of ZnO, is used to activate the vulcanization process and is also present in the brass coatings applied to the steel wires that reinforce the tire structure (Thorpe and Harrison 2008). Thus, our results support the assumption that these elements were traffic-related in the region.

Structural aspects of scales' cell and relationships with atmospheric pollutants

The occurrence of phenolic compounds was ubiquitous in leaf tissues of *T. usneoides* (Fig. 4). Phenolic compounds from trichomes, cuticle, vascular fibers, and xylem cells exhibited strong emission all over the selected emission spectra

regardless the excitation laser applied (Fig. 4a, b). On the other hand, phenolic compounds present at mesophyll cell wall exhibited a strong emission (between 410 and 560 nm) only when excited at 364 nm (Fig. 4a). Qualitatively (regarding distribution and intensity of emission), there was no differencing emissions from T0 to T9 plants. Phenolic compounds reduce the availability of metals to plant tissues and subcellular compartments by binding to metals (chelation). The widespread distribution of these compounds in *T. usneoides* tissues (visualized by their emissions from cell wall, cuticle, and scales) confers a protection to the damage effects of metals, by providing locations to their immobilization (Sakihama et al. 2002; Tangahu et al. 2011). Indeed, this characteristic of phenolic compounds in forming complexes with metals is the basis of histochemical tests to detect these compounds, as iron and aluminum chloride to in situ detection of polyphenols and flavonoids, respectively (Johansen 1940; Charriere-Ladreix 1973). The strong emission mainly from scales (but also from the ordinary epidermis cells) was related to a higher concentration of polyphenols in these structures, explaining then how this structures can adsorb metals and avoid their entrance to inner tissues. This may be the reason of the Hg adsorption at scales and absence of this metal at leaf/stem inner tissues reported by Amado Filho et al. (2002) and Vianna et al. (2011), and explains the capacity of this species to accumulate a higher concentration of metals.

The surface of *T. usneoides* leaves in frontal view was covered by scales. Each scale was constituted of a central disk composed by four cells that comprised a circle; the central disk was surrounded by the ring cells arranged in two series, the innermost consisting of 8 cells and the outermost of 16 ones. Peripherally to this last layer, 32 elongated cells were

Fig. 3 Cluster analysis of metal concentrations from control site and new road plants

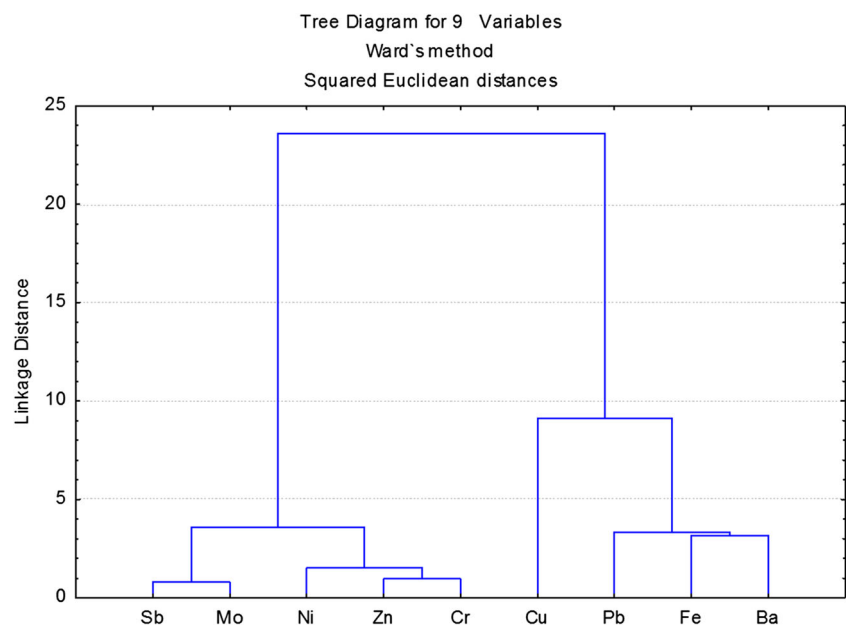
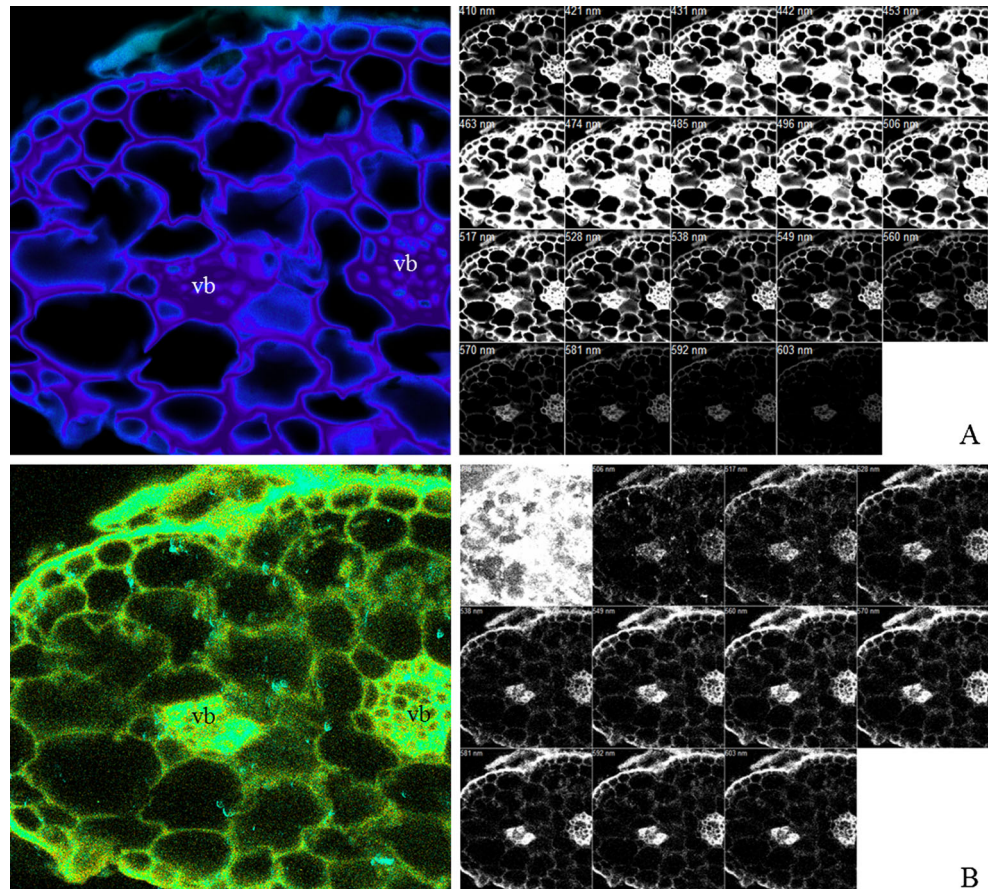


Fig. 4 Emission spectra of phenolic compounds from leaves of *Tillandsia usneoides* (samples from T9 exposure period). Lambda-stack images from leaves excited at 364 (a) and 488 nm (b) laser lines and emissions collected from 400 to 600 nm and 490 to 600 nm, respectively. Comparing both excitation lines, the 364 nm one induced an intense emission from phenolic compounds of mesophyll cell wall, while both laser lines excited these metabolites from cuticle, scales, epidermis, and vascular bundles. **b** The shiny image at 496 nm refers to the proximity of this wavelength to the 488 nm excitation. *vb* vascular bundle

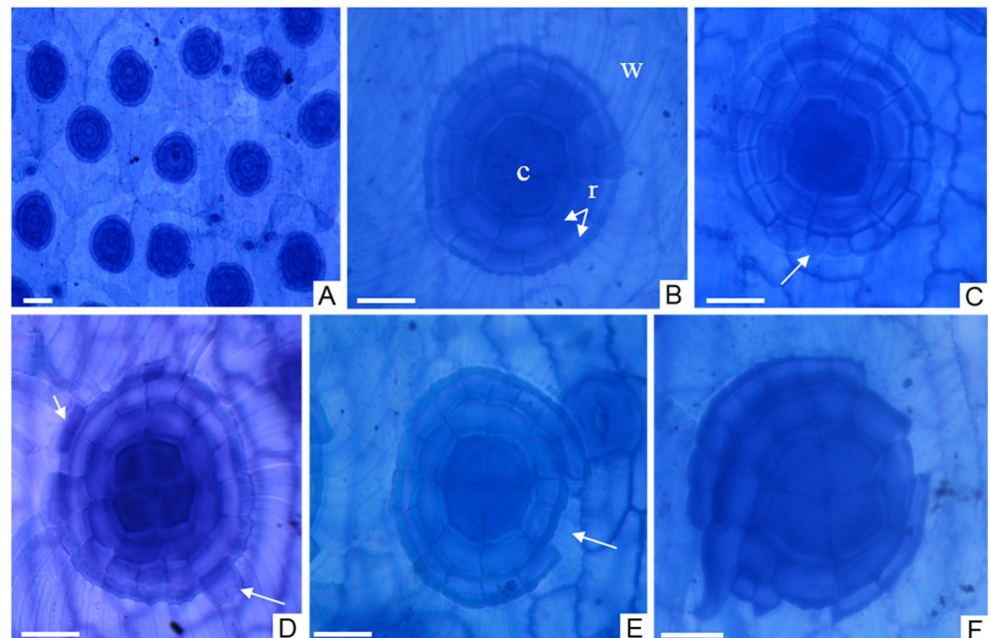


radially arranged, constituting the scale wing (Fig. 5a, b). Concerning the abnormalities observed in the number of scale cells, subtraction or addition of cells in outermost layer of the ring (Fig 5c–e), addition of cells between outermost ring and

wing cells (Fig. 5e), and changes in morphology of the ring cells (Fig. 5f) were observed.

The percentage of anomalous scales in plants exposed at the control site was significantly higher at T8 compared to the

Fig. 5 Structure and cell alterations of scales from *T. usneoides* leaves. **a–f** Paradermal surface of the leaf. **a** Overview of epidermis and scales. **b** Detail of the scale cells organization: the central disk (c), the inner and the outermost rings (r), and the scale wing (w). **c–f** Anomalous scales. **c** Addition of cells in the outermost ring (arrow). **d** Wing cells replacing the outermost ring ones (arrows). **e** Subtraction of a cell from the outermost ring (arrow). **f** Multiple abnormalities in scale cells organization. Scale bars 40 μm



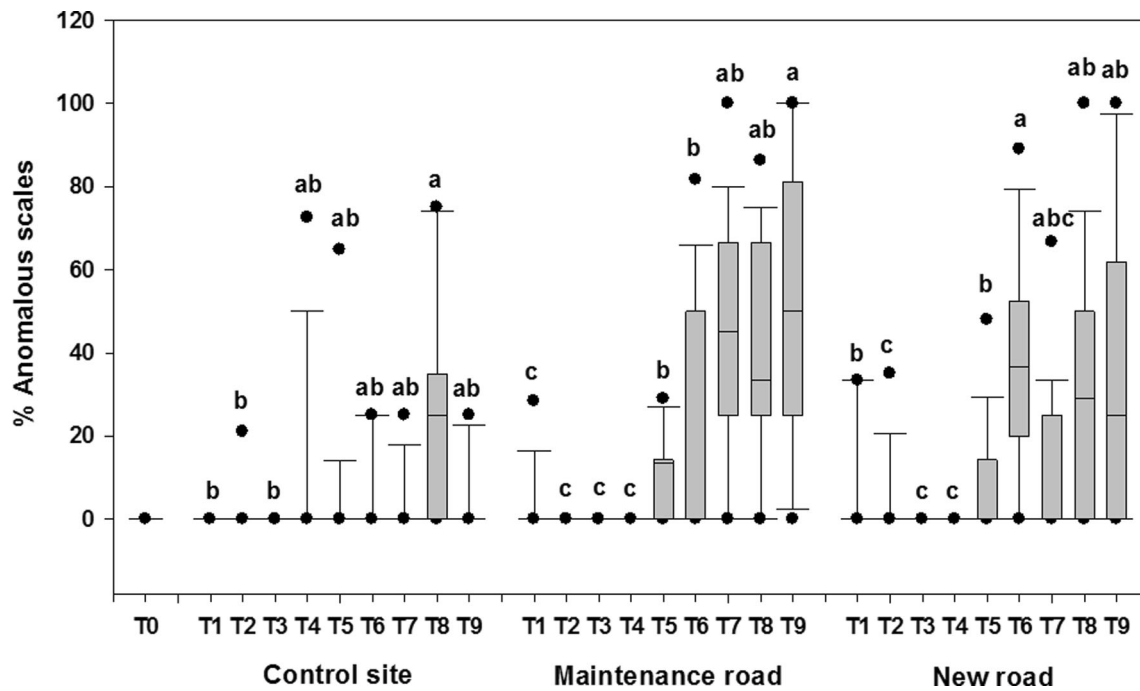


Fig. 6 Boxplot representation of anomalous scales' percentage from *Tillandsia usneoides* leaves. The rectangles delimit 25th to 75th percentiles of the original datasets, the symbols (black circle) delimit the 5th and 95th percentiles and the horizontal lines inside the

rectangles represent the median values. Distinct letters indicate significant differences among exposure times in each site (ANOVA on ranks; Dunn's test; $p < 0.05$)

estimated percentage from T1 to T3 periods. In addition, the percentage increased significantly in T5 plants kept close to maintenance road. This same tendency was observed in plants exposed close to the new road site, but showing a higher variability (Fig. 6).

A positive correlation was proved between the percentage of anomalous scales and Ba, Cu, Fe, Mo, and Ni concentrations in plants maintained in the control site. Pearson correlations were not significant at the polluted sites, except in plants from the point close to the maintenance road where the anomalous scales correlated negatively with Fe and Ba concentrations (Table 2). According to our aforementioned reasoning concerning the chelating properties of phenolic compounds, we may assume that the metals identified in plants from the polluted sites, even in high concentrations, did not promote a mutagenic effect over scale cells, contrasting with results from the control site. Thus, the results indicate that the observed scale anomalies may be attributed to other atmospheric pollutants, which are also originated by vehicular emissions, such as nitrogen and sulfur oxides, or formed by photochemical reactions, such as ozone.

The anomalies observed in the scale cells were related to alterations in both shape and number of cells, thus indicating the occurrence of some mutagenic process. In order to verify the existence of mutagenesis in these cells, we performed observations of the nuclei of (still) living scale cells. Comparing to the nucleus of an ordinary epidermal cell, some visible nuclei of mature but still living anomalous scale cells

exhibited a larger size, especially those adjacent or close to missing peripheral cells (Fig. 7). This increase in the nuclei size seemed to be caused by successive endoreduplication cycles, in which no further cell division is observed. This phenomenon is the cause of the normal development of branches observed in unicellular trichomes of *Arabidopsis*. An acute unicellular trichome presents nucleus with the same size as the other ordinary epidermal cells. However, a nucleus with an increasingly higher size is observed according to the

Table 2 Pearson correlations (R) and respective significance level (p) between the average percentage of anomalous scales and heavy metal concentrations in *T. usneoides* exposed in control and polluted sites (new and old roads) during the experimental period ($n=7$)

Metals	Control site		Maintenance road		New road	
	R	p	R	p	R	p
Ba	<i>0.78</i>	0.039	-0.72	0.139	0.16	0.707
Cu	<i>0.90</i>	0.005	-0.22	0.636	0.54	0.167
Cr	-0.50	0.370	-0.32	0.485	0.14	0.763
Fe	<i>0.86</i>	0.004	-0.81	0.030	-0.13	0.762
Mo	<i>0.96</i>	<0.001	-0.54	0.211	0.47	0.245
Ni	<i>0.91</i>	0.004	-0.09	0.841	0.66	0.106
Pb	0.42	0.342	-0.70	0.078	0.29	0.536
Sb	-0.11	0.011	0.40	0.464	0.49	0.217
Zn	0.25	0.528	0.53	0.144	0.43	0.292

Significant correlation coefficients are highlighted in italics

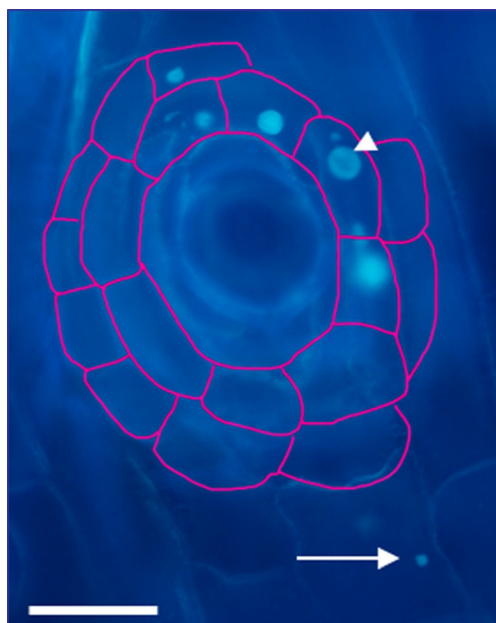


Fig. 7 DAPI-stained nucleus from epidermis and anomalous scale cells of *Tillandsia usneoides* leaf. Different sizes of nucleus from ring cells (arrowheads) compared to the one from ordinary epidermis (arrow); cell wall boundaries outlined in pink. Note that scale cells exhibit a larger nucleus size, an indicative of successive endoreduplication cycles. Scale bar 40 μm

number of developed branches (Uhrig and Hulskamp 2010). Interestingly, some mutagenic compounds can also promote alterations in the cell cycle resulting in abnormalities. Some atmospheric pollutants, such as ozone and nitrogen and sulfur oxides, do act as mutagenic agents, promoting alterations in nucleus in bacteria and humans (Hamelin and Chung 1974; Meng et al. 2004; Diler and Ergene 2010). By analogy, these gaseous pollutants, which are also constituents of São Paulo atmosphere (Molina and Molina 2004), may have induced the mutagenic effects on the scale cells in *T. usneoides* exposed in the polluted sites.

Conclusions

We applied *T. usneoides* as a broader biomonitor of atmospheric pollution (gaseous pollutants and metals) to assess the changes in air quality during the construction and opening of a highway (SP-21) in São Paulo State, Brazil. The pivotal conclusions are summarized as follows:

1. Metal analysis showed an increase in the concentration of most determined elements, the ones directly related to vehicular emissions, after the inauguration of the SP-21 highway (April/2010) indicating that they are originated from these emissions.

2. Cr and Zn in *T. usneoides* plants were adequate tracers of non-exhaust traffic-related elements.
3. Metals were chelated by phenolic compounds present mainly at scale cells, thus avoiding their entrance in inner tissues and reducing damages to the plant.
4. Anomalies in number and shape of scale cells reflected alterations in the size of nuclei, a result of successive endoreduplication cycles caused by mutagenic compounds such as ozone, nitrogen, and sulfur oxides that are also related to traffic pollution. Therefore, the percentage of anomalous scales can be used as a more embracing biomonitoring of atmospheric pollution, to detect a change in the general pollution profile induced by a new pollution source.

We recommend the use of *T. usneoides* as a wide biomonitor of air quality in urbanized areas, based on both the metal enrichment properties and anomalies in its scale cells.

Acknowledgments The authors thank Brazilian CAPES, FAPESP and CNPq for financial support, DERSA Desenvolvimento Rodoviário SA for allowing access to the SP-21 highway, Central Analítica (Instituto de Química, Universidade de São Paulo) for assistance with confocal microscopy, and Núcleo de Pesquisa em Anatomia (Instituto de Botânica) for laboratory supply and equipment.

References

Alves ES, Moura BB, Domingos M (2008) Structural analysis of *Tillandsia usneoides* L. Exposed to Air pollutants in São Paulo city—Brazil. *Water Air Soil Pollut* 189:61–68

Amado Filho GM, Andrade LR, Farina M, Malm O (2002) Hg localisation in *Tillandsia usneoides* L. (Bromeliaceae), an atmospheric biomonitor. *Atmos Environ* 36:881–887

Apeygei E, Bank MS, Spengler JD (2011) Distribution of heavy metals in road dust along an urban–rural gradient in Massachusetts. *Atmos Environ* 45:2310–23

Bettinelli M, Perotti M, Spezia S, Baffi C, Beone GM, Alberici F, Bergonzi S, Bettinelli C, Cantarini P, Mascetti L (2002) The role of analytical methods for the determination of trace elements in environmental biomonitors Piacenza, Italy. *Microchem J* 73:131–152

Cadle SH, Mulawa PA, Ball J, Donase C, Weibel A, Sagebiel JC, Knapp KT, Snow R (1997) Particulate emission rates from in-use high-emitting vehicles recruited in orange county, California. *Environ Sci Technol* 31:3405–3412

Charriere-Ladreix Y (1973) Study of the flavonoid secretion from *Populus nigra* L. var. *italica*: kinetics of secretory phenomena, ultrastructure and evolution of secretory tissues (in French). *J Microscopie* 17:299–316

Conti ME, Cecchetti G (2001) Biological monitoring: lichens as bioindicators of air pollution assessment—a review. *Environ Pollut* 114:471–492

Desenvolvimento Rodoviário SA (2015) <http://www.dersa>. Accessed:07,15, 2015

Diler BS, Ergene S (2010) Nuclear anomalies in the buccal cells of calcite factory workers. *Genet Mol Biol* 33:374–378

Duong TTT, Lee B (2011) Determining contamination level of heavy metals in road dust from busy traffic areas with different characteristics. *J Environ Manag* 92:554–562

- Figueiredo AMG, Nogueira CA, Saiki M, Milian FM, Domingos M (2007) Assessment of atmospheric metallic pollution in the metropolitan region of São Paulo, Brazil, employing *Tillandsia usneoides* L. as biomonitor. *Environ Pollut* 145:279–292
- Gunawardana C, Goonetilleke A, Egodawatta P, Dawes L, Kokot S (2012) Source characterisation of road dust based on chemical and mineralogical composition. *Chemosphere* 87:163–170
- Hamelin C, Chung YS (1974) Optimal conditions for mutagenesis by ozone in *Escherichia coli* K12. *Mutat Res Fund Mol Mech* 24:271–279
- Isaac-Olivé K, Solís C, Martínez-Carrillo MA, Andrade E, López C, Longoria LC, Lucho-Constantino CA, Beltrán-Hernández RI (2012) *Tillandsia usneoides* L, a biomonitor in the determination of Ce, La and Sm by neutron activation analysis in an industrial corridor in central Mexico. *Appl Radiat Isot* 70:589–594
- ISO/TC69 (2005) Statistical methods for use in proficiency testing by interlaboratory comparisons ISO 13528:2005. International Organization for Standardization (ISO), Geneva, Switzerland
- Janssen NAH, Mansom DFM, van der Jagt K, Harssema H, Hoek G (1997) Mass concentration and elemental composition of airborne particulate matter at street and background locations. *Atmos Environ* 31:1185–1193
- Johansen DA (1940) *Plant microtechnique*. McGraw-Hill Books, New York
- Liu E, Yan T, Gavin B, Zhu Y (2014) Pollution and health risk of potentially toxic metals in urban road dust in Nanjing, a mega-city of China. *Sci Total Environ* 476–477:522–531
- Loppi S, Bonini I (2000) Lichens and mosses as biomonitors of trace elements in areas with thermal springs and fumarole activity (Mt. Amiata, central Italy). *Chemosphere* 41:1333–1336
- Meng Z, Qin G, Zhang B, Bai J (2004) DNA damaging effects of sulfur dioxide derivatives in cells from various organs of mice. *Mutagenesis* 19:465–468
- Metcalfe CR, Chalk L (1979) *Anatomy of dicotyledons*, 2nd edn. Clarendon, Oxford
- Modrzewska B, Wyszowski M (2014) Trace metals content in soils along the state road 51 (northeastern Poland). *Environ Monit Assess* 186:2589–2597
- Molina MJ, Molina LT (2004) Megacities and atmospheric pollution. *J Air Waste Manage Assoc* 54:644–680
- Monaci F, Moni F, Lanciotti E, Grechi D, Bargagli R (2000) Biomonitoring of airborne metals in urban environments: new tracers of vehicle emission, in place of lead. *Environ Pollut* 107:321–327
- Ribeiro AP, Figueiredo AMG, Ticianelli RB, Nammoura-Neto GM, Silva NC, Kakazu M, Zahn G (2012) Metals and semi-metals in street soils of São Paulo city, Brazil. *J Radioanal Nucl Chem* 291:137–142
- Saiki M, Santos JO, Alves ER, Genezini FA, Marcelli MP, Saldiva PHN (2014) Correlation study of air pollution and cardio-respiratory diseases through NAA of an atmospheric pollutant biomonitor. *J Radioanal Nucl Chem* 299:773–779
- Sakihama Y, Cohen MF, Grace SC, Yamasaki H (2002) Plant phenolic antioxidant and prooxidant activities: phenolics-induced oxidative damage mediated by metals in plants. *Toxicology* 177:67–80
- Tangahu BV, Abdullah SRS, Basri H, Idris M, Anuar N, Mukhlisin M (2011) A review on heavy metals (As, Pb, and Hg) uptake by plants through phytoremediation. *Int J Chem Eng* 939161
- Techato K, Salaeh A, van Beem NC (2014) Use of atmospheric epiphyte *Tillandsia usneoides* (Bromeliaceae) as biomonitor. *APCBEE Procedia* 10:49–53
- Thorpe A, Harrison RM (2008) Sources and properties of non-exhaust particulate matter from road traffic: a review. *Sci Total Environ* 400:270–282
- Uhrig JR, Hulskamp M (2010) Trichome development in *Arabidopsis*. *Plant Dev Biol* 655:77–88
- Vianna NA, Gonçalves D, Brandão F, Barros RP, Amado Filho GM, Meire RO, João PM, Torres JPM, Malm O, D'Oliveira Júnior A, Andrade LR (2011) Assessment of heavy metals in the particulate matter of two Brazilian metropolitan areas by using *Tillandsia usneoides* as atmospheric biomonitor. *Environ Sci Pollut Res* 18:416–427
- Zechmeister HG, Hohenwallner D, Riss A, Hanus-Ilmar A (2005) Estimation of element deposition derived from road traffic sources by using mosses. *Environ Pollut* 138:238–249